MODELING OF HEAT TRANSFER IN AN ISOTROPIC VELOCITY FIELD IN THE PRESENCE OF A TRANSVERSE TEMPERATURE GRADIENT

B. A. Kolovandin and N. N. Luchko

UDC 532.517.4

Known second-order models are verified in a test problem of an isotropic velocity field with a constant temperature gradient.

Despite the extensive utilization of second-order velocity field models for the solution of practical shear turbulence problems (for instance, the $k - \varepsilon_u$ Launder model, etc. [1]), up to now no equivalents are known in completeness of description and incontrovertibility of the experimental data of the second-order model of an inhomogeneous scalar field. Known attempts of the construction of such models are limited to the simplest form of scalar field turbulence being realized in the wake behind a heated grating. The velocity field in such a flow is described by the system of equations

$$\frac{dq^2}{dt} = -2\varepsilon_u,$$
$$\frac{d\varepsilon_u}{dt} = -F_u \frac{\varepsilon_u^2}{q^2}, \tag{1}$$

where the coefficient F_u equals 11/3 for strong turbulence ($R_\lambda \to \infty$). The rms value of the scalar fluctuation is here described by the equation

$$\frac{d\overline{c^2}}{dt} = -2\varepsilon_c. \tag{2}$$

An equation for ε_c in the form

$$\frac{d\varepsilon_c}{dt} = -\Psi \frac{\varepsilon_c}{\tau_\varepsilon}, \tag{3}$$

was proposed in [2-3], where the time scale τ_ε was either taken equal to the velocity field scale $\tau_\varepsilon = \tau_{\varepsilon u} = q^2/\varepsilon_u$ or the scalar field scale $\tau_\varepsilon = \tau_{\varepsilon c} = \overline{c^2}/\varepsilon_c$. As experimental data accumulated, generalized in [4], the unsatisfactoriness of (3) was shown. The mentioned Warhaft and Lumley paper initiated a number of theoretical and numerical investigations on modeling a degenerating isotropic scalar field. Thus, an equation for ε_c in the form

$$\frac{d\varepsilon_c}{dt} = -\Psi_1 \frac{\varepsilon_c}{\tau_{\varepsilon u}} - \Psi_2 \frac{\varepsilon_c}{\tau_{\varepsilon c}}, \tag{4}$$

was proposed in [5-7], where the coefficients equal 5/3 and 2, respectively, as $R_\lambda \to \infty$ and $P_\lambda \to \infty$, which satisfactorily described (in combination with (2) and (1)) the dynamics of a scalar field behind a heated "mandolin" placed in the wake behind a turbulent grating.

In the general case of an inhomogeneous scalar field, the equations for $\overline{c^2}$ and ε_c as well as the equation for the stream $\overline{u_2 c}$ contain a number of unknown terms, whose formal definition is possible only to the accuracy of the time scales. To analyze the adequacy of a "closed" model of a flow with the gradient of an averaged scalar value in which the inhomogeneous turbulence of a scalar field is formulated, it is expedient to confirm the model in test flows including a small quantity of turbulent transfer factors.

The simplest form of an inhomogeneous field of a passive scalar is realized in an isotropic velocity field degenerating in the flow direction x_1 in the presence of a constant gradient of the average value of the scalar $\beta = -d\bar{C}/dx_2$ = const transverse to the stream. Sirivat and Warhaft [8] performed a detailed experimental investigation of the dynamics of

A. V. Lykov Institute of Heat and Mass Transfer, Academy of Sciences of the Belorussian SSR, Minsk. Translated from Inzhenerno-Fizicheskii Zhurnal, Vol. 54, No. 1, pp. 14-20, January, 1988. Original article submitted September 29, 1986.

0022-0841/88/5401-0008 $12.50

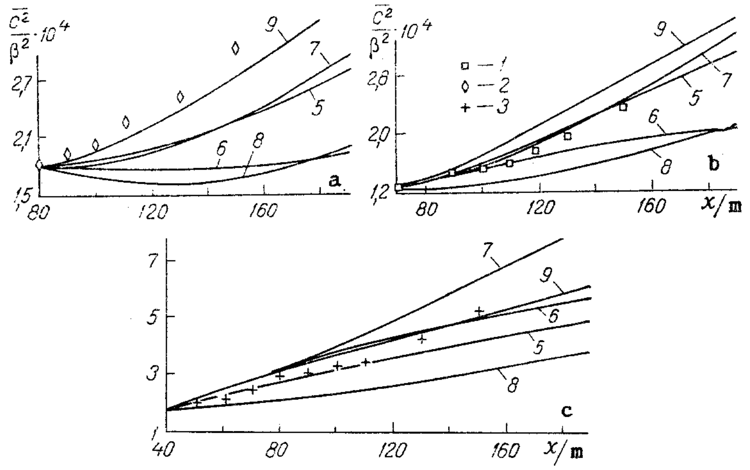

Fig. 1. Downstream change in the rms temperature fluctuations $\bar{c}^2/\beta^2$: 1, 2, 3) experiment [8]; solid lines are computation; numbers on the computed curves correspond to numbering of the formulas in the text; "mandolin" geometry (i, j) and gradient of the average temperature value β are the following: a) (10.1); $\beta = 2.24$°C/m; b) (2.2); $\beta = 1.78$°C/m; c) (2.1); $\beta = 7.48$°C/m. $\bar{c}^2/\beta^2 \cdot 10^4$ m².

a scalar field in such a flow. The formulation of known second order models for the evolution of the scalar field under consideration has the following form for $R_\lambda \gg 1$ and $P_\lambda \gg 1$.

A model of the first author of the present paper (its detailed exposition is contained in [9] for the general case of inhomogeneous velocity fields and a passive scalar)

$$\frac{d\overline{u_2c}}{dt} = \frac{1}{3}\beta q^2 - \frac{1}{3}\frac{m}{m-9P_c}\left(\frac{1}{\tau_{\varepsilon u}} - \frac{6P_c - n}{\tau_{\varepsilon c}}\right)\overline{u_2c},$$

$$\frac{d\varepsilon_c}{dt} = 2\,\frac{m-9P_c-1}{m-9P_c}\,\beta\,\frac{\overline{u_2c}}{\tau_{\varepsilon c}} - 2\,\frac{\varepsilon_c}{\tau_{\varepsilon c}} - \frac{1}{3}\,\frac{5m-54P_c}{m-9P_c}\,\frac{\varepsilon_c}{\tau_{\varepsilon u}}, \tag{5}$$

$$m = 1{,}5n + 1, \quad n = 10;$$

the Lumley model [10]

$$\frac{d\overline{u_2c}}{dt} = \frac{1}{3}\beta q^2 - \left[1 + R + 1{,}1R^2\sqrt{\frac{1-\rho^2}{(1-\rho^2/3)^3}}\right]\frac{\overline{u_2c}}{\tau_{\varepsilon u}},$$

$$\frac{d\varepsilon_c}{dt} = -\left(2 + \frac{9}{5}\,\frac{1}{R} - 2{,}05P_c\right)\frac{\varepsilon_c}{\tau_{\varepsilon c}}; \tag{6}$$

the Élgobashi and Launder model [11]

$$\frac{d\overline{u_2c}}{dt} = \frac{1}{3}\beta q^2 - 4{,}3\,\frac{\overline{u_2c}}{\tau_\varepsilon},$$

$$\frac{d\varepsilon_c}{dt} = 1{,}8\beta\,\frac{\overline{u_2c}}{\tau_{\varepsilon c}} - 2{,}2\,\frac{\varepsilon_c}{\tau_{\varepsilon c}} - 1{,}6\,\frac{\varepsilon_c}{\tau_{\varepsilon u}}, \quad \tau_\varepsilon = \tau_{\varepsilon c} = \overline{c^2}/\varepsilon_c; \tag{7}$$

the Élgobashi and Launder model [11]

$$\frac{d\overline{u_2c}}{dt} = \frac{1}{3}\beta q^2 - 8{,}6\,\frac{\overline{u_2c}}{\tau_\varepsilon}, \tag{8}$$

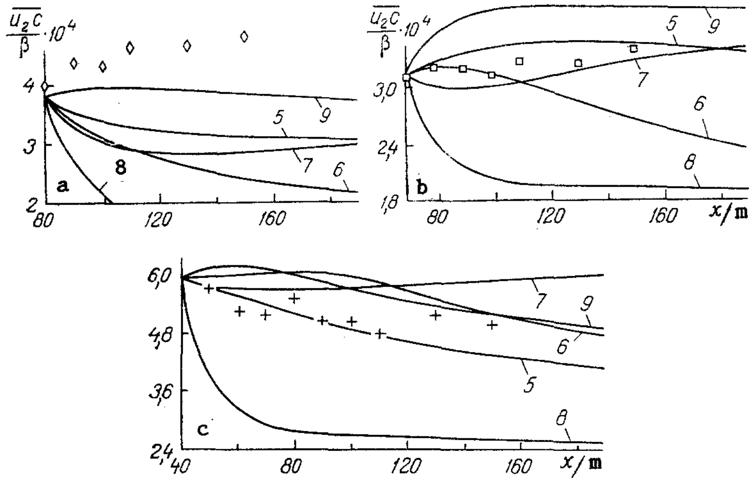

Fig. 2. Downstream change in the transverse heat flux $\overline{u_2c}/\beta$; notation the same as in Fig. 1. $\overline{u_2c}/\beta\cdot 10^4$ m^2/sec.

$$\frac{d\varepsilon_c}{dt} = 1{,}8\beta\,\frac{\overline{u_2c}}{\tau_{\varepsilon c}} - 2{,}2\,\frac{\varepsilon_c}{\tau_{\varepsilon c}} - 1{,}6\,\frac{\varepsilon_c}{\tau_{\varepsilon u}}, \quad \tau_\varepsilon = \sqrt{\tau_{\varepsilon u}\tau_{\varepsilon c}};$$

the model of the second author of this paper (see also [9])

$$\frac{d\overline{u_2c}}{dt} = \frac{1}{3}\beta q^2 - \beta\,\frac{(\overline{u_2c^2})}{\overline{c^2}} - (1+R)\frac{\overline{u_2c}}{\tau_{\varepsilon u}},$$
$$\frac{d\varepsilon_c}{dt} = -\frac{5}{3}\,\frac{\varepsilon_c}{\tau_{\varepsilon u}} - 2\,\frac{\varepsilon_c}{\tau_{\varepsilon c}} + \frac{4+7R}{5}\,\beta\,\frac{\overline{u_2c}}{\tau_{\varepsilon u}}, \tag{9}$$

where $P_c = \beta\overline{u_2c}/\varepsilon_c$ is a parameter of the ratio between the generation velocity $\overline{c}^2$ because of the gradient of the average value of the scalar and the velocity of "dissipation" ε_c; $R = \tau_{\varepsilon u}/\tau_{\varepsilon c}$ is the parameter of the ratio between the time scales of the velocity fluctuation and the scalar substance, $\rho = u_2c/\sqrt{\overline{u_2^2}\,\overline{c^2}}$ is the correlation coefficient of the transverse velocity fluctuations and the scalar. The rms value of the scalar fluctuations is here described by the equation

$$\frac{d\overline{c^2}}{dt} = 2\beta\overline{u_2c} - 2\varepsilon_c, \tag{10}$$

and the velocity field parameters are determined by the system (1).

The differences, in principle, between the models presented above are the different modes of approximating the "dissipative" term in the equation for the stream u_2c and the term characterizing generation of the parameter ε_c because of the scalar substance gradient in the equation for ε_c (different approaches to the approximation of these terms and the determination of the constant by the models are contained in the original papers [9-11]).

On the basis of the models (5)-(9) a numerical modelling of the experiment [8] to estimate the degree of adequacy of the reflection of the effect of the gradient of the average value of the scalar by the models under consideration in the dynamics of the fluctuating characteristics of the scalar.

The Cauchy problem for the system (1) of the velocity field and (5)-(9), (10) of the scalar field was posed for identical initial conditions for each model, which were borrowed from experiment [8], for the "mandolin." It should be noted that giving the initial conditions for the scalar field parameters corresponding to experiment is not trivial. Indeed, the field of scalar fluctuations in direct proximity to the "mandolin" is determined mainly by the geometry of the "mandolin," i.e., by local gradients of the average value of the scalar at the dimensions of hot jets. On the other hand, the models (5)-(9) are formulated under the assumption that the scalar fluctuations are generated just by a linear gradient

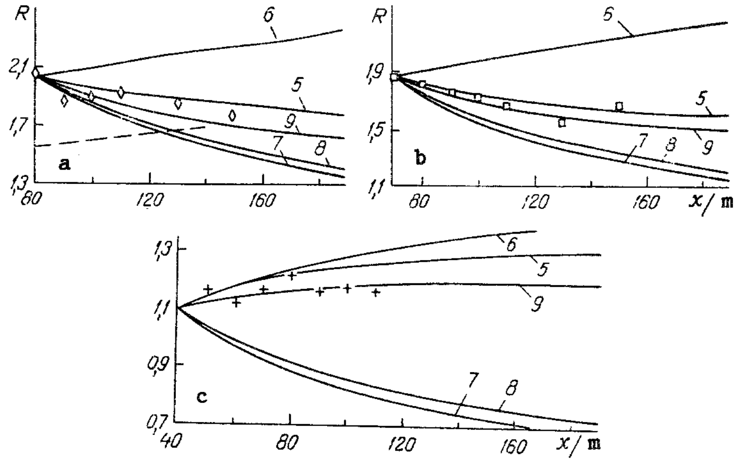

Fig. 3. Downstream change in the parameters of the scale ratio R; notation the same as in Fig. 1.

β transverse to the stream in the whole domain being considered. Therefore, the initial conditions for the Cauchy problem should be selected from experiment for sufficiently large distances from the "mandolin" for which the linear gradient of the average value of the scalar was known to be formulated. However, these distances should not be so great that the parameters ρ and R would become close to their asymptotic values (if such exist).

In connection with the mentioned singularity of formation of the scalar fluctuation field, experimental data for the evolution of the energetic spectrum of the scalar fluctuation would be desirable in the experiment [8] for the well-founded selection of the initial conditions in the numerical modeling. Since there are no such data in [8], the value of the dimensionless longitudinal coordinate x_1/M at which the influence of the first term in the right side of (10) would approximately equal the second term was selected the point of the beginning of the numerical counting for each "mandolin" geometry. Starting with this point, the generation of the parameter $\bar{c}^2$ because of the transverse gradient β exceeds its molecular "dissipation."

Results of a computation of the evolution of the temperature fluctuation intensity $\bar{c}^2$ in the longitudinal x_1/M coordinate, the transverse heat flux $\overline{u_2 c}$, and the scale ratio parameter R for different "mandolin" geometries (i, j)* and different values of the transverse gradient of the average value of the temperature $\bar{C}$ are presented in Figs. 1-3. Comparison of the computed and experimental data shows that the Launder and Élgobashi model (8) with the hybrid time scale $\tau_\varepsilon = \sqrt{\tau_{\varepsilon u}\tau_{\varepsilon c}}$ in the equation for the flux $\overline{u_2 c}$ does not possess either quantitative or qualitative adequacy for the experiment. The model (7) of these same authors describes only the parameters $\bar{c}^2$ and $\overline{u_2 c}$ satisfactorily just for the "mandolin" geometry (2.2). As regards the scale ratio parameter R, the models mentioned demonstrate a rate of its change in x_1/M that is opposite to experiment.

The Lumley model (6) yields somewhat better agreement with experiment than the Élgobashi and Launder model, however, not as superior as is shown in [10]. The fact is that the initial conditions for the parameter ε_c (and therefore for R) were not given from the Sirivat and Warhaft experiment in the paper mentioned but were determined from the condition of best agreement between the computed and experimental data for $\bar{c}^2$ and $\overline{u_2 c}$. In particular, superior agreement is observed (see Fig. 4) between the results of a computation by the Lumley model and the data of an experiment for a "mandolin" (10, 1) (the other models under consideration, with the exception of the model (8), also yield satisfactory agreement with experiment) when the parameter r is given at the point x_1/M equal to the experimental value diminished 1.5 times (see Fig. 4). However, the evolution of the parameter R (the dashed line in Fig. 3a) here describes the experimental data poorly.

As regards models (5) and (9) of the authors of this paper, they yield approximately identical agreement between the computed and experimental results, with the exception of the version (10, 1).

---

* The Sirivat and Warhaft [8] notation is used here: i is the dimensionless distance (referred to the size of the grating cell) of the "mandolin" from the grating, while the index j is the dimensionless distance between "mandolin" wires.

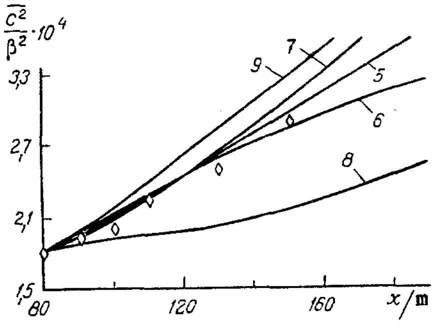

Fig. 4. Downstream change in the rms temperature fluctuations $\overline{c^2}/\beta^2$ for an initial value of the parameter R diminished 1.5 times as compared with the experimental value; notation the same as in Fig. 1; (10, 1); $\beta = 2.24°C/m$. $\overline{c^2}/\beta^2 \cdot 10^4$ m^2.

DISCUSSION OF THE RESULTS

Known second-order models of a scalar field are examined in this paper in a test problem on the development of temperature fluctuations in the wake behind a grating during the imposition of a constant gradient of the average temperature value transverse to the stream on an almost isotropic degenerating velocity field.

The selection of this problem was governed firstly by the fact that the scalar field generated by the linear transverse gradient of the average scalar value is the simplest prepresentative of an inhomogeneous field not subjected to turbulent diffusion. This problem allows direct investigation of the sensitivity of the model to the generation of a turbulent scalar field because of the transverse gradient of an average scalar value. Secondly, the dynamics of an inhomogeneous scalar field of this kind is documented well by a careful experiment [8]. However, the incomplete conformity of the mathematical formulation of the problem to the experiment should be noted. It was assumed in the formulation of the problem that the transverse constant gradient β is the single generator of the scalar field fluctuations. Two temperature fluctuation generators are actually present in the experiment: the "mandolin" strings shaping relatively fine-scale temperature fluctuations, and the transverse gradient β that generate relatively coarse-scale fluctuations. Therefore, two fluctuating scalar fields are realized in the experiment with different characteristic length scales. At sufficiently large distances from the "mandolin" the factor of the transverse gradient β becomes dominant in the generation of $\overline{c^2}$, i.e., a scalar field is realized with one characteristic scale. The nonconformity of the experiment data with the computation by the models considered above, which are single-scale, is explained certainly by the scalar field realized in experiment being two-scale, especially for a "mandolin" significantly remote from the grating (for instance, the geometry (10, 1)). The characteristic length scale of a fluctuating scalar field in these models is either the Taylor scale $\lambda_c = \sqrt{6\kappa\overline{c^2}/\varepsilon_c}$ or the scale of the energy containing scalar "vortices" $L_c = 6q\overline{c^2}/\varepsilon_c$, or the time scale $\tau_{\varepsilon c} = \overline{c^2}/\varepsilon_c$.

Therefore, with the exception of the geometry (10, 1) for which a two-scale scalar field is apparently realized in experiment (at least at distances x_1/M achieved in the experiment), the most satisfactory agreement between the computed and experimental data is obtained for the models (5) and (9). The model (5) developed (see [9]) for inhomogeneous velocity fields in the general case and a passive scalar for arbitrary values of the Reynolds and Peclet turbulence numbers and the Prandtl molecular number, needs further examination in test problems for fields of more complex shape.

NOTATION

u_i, velocity fluctuation component; $q^2 = \overline{u_i^2}$, twice the turbulence kinetic energy; t, time; x_i, Cartesian coordinates; $\varepsilon_u = \nu\overline{(\partial u_i/\partial x_k)^2}$, rate of dissipation of the turbulence kinetic energy; $\bar{C}$, average scalar value; c, scalar fluctuation; $\overline{c^2}$, rms value of the scalar fluctuation, $\varepsilon_c = \kappa\overline{(\partial c/\partial x_k)^2}$, rate of "blurring" of the scalar fluctuation; $\lambda_u = \sqrt{5\nu q^2/\varepsilon_u}$, $\lambda_c = \sqrt{6\kappa\overline{c^2}/\varepsilon_c}$, microscales of the vector and scalar fields; $R_\lambda = q\lambda_u/\nu$, $P_\lambda = q\lambda_c/\kappa$, turbulent Reynolds and Peclet numbers; $\tau_{\varepsilon u} = q^2/\varepsilon_u$, $\tau_{\varepsilon c} = \overline{c^2}/\varepsilon_c$, gradient of the average scalar value; and M, characteristic grating size.

LITERATURE CITED

1. B. E. Launder, G. J. Reece, and W. Rodi, J. Fluid Mech., 68, 537-566 (1975).
2. J. L. Lumley, Int. Symp. Strat. Flows (Novosibirsk, 1972), 333-341, Novosibirsk (1972).

3. B. A. Kolovandin and J. A. Vatutin, Int. J. Heat Mass Transfer, 15, 2371-2383 (1972).
4. Z. Warhaft and J. L. Lumley, J. Fluid Mech., 88, 659-684 (1978).
5. G. R. Newman, B. E. Launder, and J. L. Lumley, J. Fluid Mech., 111, 217-232 (1981).
6. B. A. Kolovandin and N. N. Luchko, Dokl. Akad. Nauk BSSR, 25, No. 7, 601-604 (1981).
7. B. A. Kolovandin and N. N. Luchko, Lett. Heat Mass Transfer, 8, 321-328 (1981).
8. B. A. Sirivat and Z. Warhaft, J. Fluid Mech., 128, 323-346 (1983).
9. B. A. Kolovandin, Modeling the Dynamics of Turbulent Heat and Mass Transfer Processes Preprint No. 18, Inst. Heat Mass Transfer, Beloruss. Acad. Sci., Minsk (1986).
10. T.-H. Shih and J. L. Lumley, J. Fluid Mech., 162, 211-222 (1986).
11. S. E. Elgobashi and B. E. Launder, Phys. Fluids, 26, No. 9, 2415-2419 (1983).

VERTICAL DISPERSION OF INTENSIVE SHEAR FLOWS OF LOW-VISCOSITY FLUIDS

V. V. Gil', R. Dzhoshi,
V. L. Kolpashchikov, S. A. Kuleshov,
O. G. Martynenko, and A. I. Shnip

UDC 532.525.2

The method of high-speed visualization is used in conjuction with Doppler-laser anemometry to conduct an experimental study of the behavior of cylindrical jet of a low-viscosity fluid. A mechanism is proposed for the vertical dispersion of the fluid and is substantiated.

A jet travelling at moderate velocities decays under the influence of capillary forces. Rayleigh [1] examined a cylindrical jet the surface of which was subjected to as small a disturbance as desired. The source of the initial disturbance, meanwhile, can be either inside the channel (roughness, turbulence in the fluid, etc.) or outside (movement of the air surrounding the jet). The main characteristics of the jet decay process in this case are the length of its continuous part and the size of the drops which are formed. According to Rayleigh, the surface of the jet is unstable against disturbances with different wavelengths, but there is a wavelength at which pulsations in a jet with a free surface lead to its decay and disintegration into drops of a size on the same order of this wavelength $\lambda_{max} = 9.027$. Following Rayleigh, most investigators have maintained that, given sufficiently high discharge velocities, drops are formed due to instability of the jet surface against wavy disturbances as a result of an increase in the intensity of these perturbations. Here, we examine wave formation on the surface of a fluid with allowance for the dynamic effect of the gaseous medium on the surface of the jet. In well-known recent investigations ([2-4, etc.]), the transition from Rayleigh decay to atomization is described by means of laws governing the interaction of a gas with the surface of a free jet and the development of surface oscillations. These theories are based on the presence of a continuous jet section immediately adjacent to the nozzle orifice even at high discharge velocities. In our opinion, the kinetic energy of the gas transmitted to the liquid in the jet is also a source of dissipation and the formation of a new surface, i.e., the interaction of the external gaseous medium with the flow of liquid from the nozzle is the deciding factor in the decay process. Other investigators are not convinced that there is a continuous section even for moderate discharge velocities [5]. It is therefore of special interest to develop a method and conduct experiments which will make it possible to reliably determine the flow pattern at the nozzle outlet. The development of laser methods of diagnosis – in particular, Doppler-laser anemometry – and methods for high-speed visualization of two-phase flows makes it possible to conduct such studies. The diagnostic apparatus should have a high resolving power with respect to space and time and allow measurement of the velocity distribution in the cross section of the jet both at the orifice of the nozzle and in other characteristic sections. The equipment should also permit determination of the character of the drop-size distribution in these sections.

A. V. Lykov Institute of Heat and Mass Transfer, Academy of Sciences of the Belorussian SSR, Minsk. Translated from Inzhenerno-Fizicheskii Zhurnal, Vol. 54, No. 1, pp. 20-25, January, 1988. Original article submitted October 1, 1986.

0022-0841/88/5401-0013 $12.50